Biochimica et Biophysica Acta 1798 (2010) 266–274

Contents lists available at ScienceDirect

Biochimica et Biophysica Acta

journal homepage: www.elsevier.com/locate/bbamem

Review

A solid-state NMR study of the structure and dynamics of the myristoylated N-terminus of the guanylate cyclase-activating protein-2

Stephan Theisgen [a], Holger A. Scheidt [a,b], Alvicler Magalhães [c], Tito J. Bonagamba [d], Daniel Huster [a,*]

[a] Institute of Medical Physics and Biophysics, University of Leipzig, Härtelstr. 16-18, D-04107 Leipzig, Germany
[b] Institute of Biochemistry/Biotechnology, Martin Luther University Halle-Wittenberg, D-06120 Halle, Germany
[c] Instituto de Química, UNICAMP, Caixa Postal 6154, CEP 13084-971, Campinas, São Paulo, Brazil
[d] Instituto de Física de São Carlos, Universidade São Paulo, Caixa Postal 369, CEP 13560-970, São Carlos, São Paulo, Brazil

ARTICLE INFO

Article history:
Received 27 April 2009
Received in revised form 16 June 2009
Accepted 29 June 2009
Available online 17 July 2009

Keywords:
Lipid modification
GCAP-2
Membrane-peptide interaction
MAS NMR
Order parameter

ABSTRACT

Guanylate cyclase-activating protein-2 (GCAP-2) is a retinal Ca^{2+} sensor protein. It plays a central role in shaping the photoreceptor light response and in light adaptation through the Ca^{2+}-dependent regulation of the transmembrane retinal guanylate cyclase (GC). GCAP-2 is N-terminally myristoylated and the full activation of the GC requires this lipid modification. The structural and functional role of the N-terminus and particularly of the myristoyl moiety is currently not well understood. In particular, detailed structural information on the myristoylated N-terminus in the presence of membranes was not available. Therefore, we studied the structure and dynamics of a 19 amino acid peptide representing the myristoylated N-terminus of GCAP-2 bound to lipid membranes by solid-state NMR. ^{13}C isotropic chemical shifts revealed a random coiled secondary structure of the peptide. Peptide segments up to Ala_9 interact with the membrane surface. Order parameters for Cα and side chain carbons obtained from DIPSHIFT experiments are relatively low, suggesting high mobility of the membrane-associated peptide. Static ^2H solid-state NMR measurements show that the myristoyl moiety is fully incorporated into the lipid membrane. The parameters of the myristoyl moiety and the DMPC host membrane are quite similar. Furthermore, dynamic parameters (obtained from ^2H NMR relaxation rates) of the peptide's myristic acid chain are also comparable to those of the lipid chains of the host matrix. Therefore, the myristoyl moiety of the N-terminal peptide of GCAP-2 fills a similar conformational space as the surrounding phospholipid chains.

Contents

Abbreviations: GC, guanylate cyclase; GCAP-2, guanylate cyclase-activating protein-2; NCS, neuronal calcium sensor; CP MAS, cross-polarization magic angle spinning; HetCor, heteronuclear correlation; DIPSHIFT, dipolar coupling and chemical shift; DMPC, 1,2-dimyristoylphosphocholine

* Corresponding author. Tel.: +49 341 97 15701; fax: +49 341 97 15709.
E-mail address: daniel.huster@medizin.uni-leipzig.de (D. Huster).

0005-2736/$ – see front matter © 2009 Elsevier B.V. All rights reserved.
doi:10.1016/j.bbamem.2009.06.028

1. Introduction

The guanylate cyclase-activating proteins (GCAPs) are neuronal Ca^{2+}sensors (NCS) and belong to the super family of four EF-hand Ca^{2+}-binding proteins. A common feature of all NCS proteins is that their first EF-hand is not able to bind Ca^{2+} due to a conserved proline residue in the loop region of the EF-hand [1]. In GCAPs all the remaining EF-hands bind Ca^{2+} ions. The human genome encodes for at least three GCAP isoforms (GCAP1-3) [2–6], which are expressed only in the retina [7]. GCAP-1 and GCAP-2 are present in rod as well as in cone photoreceptor cells, whereas GCAP-3 is only expressed in cones [8]. GCAP-1 and GCAP-2 play a central role in light adaptation during phototransduction through the Ca^{2+}-dependet regulation of retinal guanylate cyclases (GCs).

GCAP-1 and GCAP-2 undergo a Ca^{2+}-level dependent "activator–inhibitor" transition. They inhibit both isoforms of the retinal guanylate cyclase (GC-1 and GC-2) at high Ca^{2+} concentrations typical for the dark state and activate them when the Ca^{2+} level decreases after phototransduction. Each GCAP is able to activate GC-1 and GC-2, so the individual role of each GCAP isoform is not yet fully understood [9]. The Ca^{2+} affinities for GCAP-1 and GCAP-2 are within the physiological range but only at intracellular concentrations of Mg^{2+}. Because of the about seven-fold different Ca^{2+}-binding affinities for the GC activation of GCAP-1 compared to GCAP-2, a "Ca^{2+} relay" model, in which both GCAPs would be required to function over the physiological range of Ca^{2+} concentration, was proposed. This joint action would lead to an expanded response range without losing the sensitivity-based cooperative effect of the Ca^{2+}binding on the GC regulation [10].

Like most other NCS proteins, GCAPs are N-terminally acylated [11]. N-terminal fatty acylation is the covalent attachment of a myristic acid or related fatty acids to the α-amino group of an N-terminal glycine through an amide bond. N-terminal fatty acylation is carried out cotranslationally by the myristoyl-CoA/protein N-myristoyltransferase (E.C.2.3.1.97), also known as N-terminal myristoyltransferase [12–14]. In tissues other than the retina, the proteins are homogenously acylated by myristic acid; therefore, the lipid modification is often referred to as N-terminal myristoylation. However, in photoreceptor cells modified proteins are heterogeneously acylated; for bovine GCAP an amount of 13% lauric acid (12:0), 7% myristic acid (14:0) and 30% 5-*cis*-tetradecenoic acid (14:1*n*-9) and 50% 5-*cis*,8-*cis*-tetradecadienoic acid (14:2*n*-6) was found [11]. Comparative studies between myristoylated and nonmyristoylated GCAPs revealed differences in GCAP-1 and GCAP-2. Whereas myristoylation of GCAP-2 has no influence on the affinity for the GC-1, GCAP-1 shows a seven-fold higher affinity to the GC-1 in the myristoylated state [15].

Even though myristoylation is not required for GC activation, the myristoylated forms are more effective activators of the GC [16]. In fact, the structural and functional role of the N-terminus and particularly of the myristoyl moiety is not well understood. The main reason is a lack of structural information. Currently, the structure of Ca^{2+}-bound non-myristoylated GCAP-2 (solved by solution NMR spectroscopy) is available [1], as well as the crystal structure of GCAP-3 [17]. Recently, the first structure of a myristoylated GCAP (Ca^{2+}-bound myristoylated GCAP-1) was solved by X-ray crystallography and revealed that the myristoyl moiety is completely buried within the N-terminal domain and has probably a structure stabilizing function [18]. Recent solution NMR data in the absence of lipid membranes appear to confirm this result [19]. But until today there is no structural information about any GCAP bound to, or at least in the presence of a membrane. That is because standard techniques for structural investigations like X-ray crystallography and solution NMR spectroscopy usually fail to resolve structural information in the membrane environment [20]. By contrast, solid-state NMR is capable of resolving structural information at least for membrane-bound peptides, as demonstrated for numerous examples in the past [21–28] or recently for the lipid-modified Ras peptides [29,30].

With the limited set of structural data, the role of the myristoylation of GCAP remains speculative although a general membrane association of the protein is described [31]. From the structural information available so far, three major roles of the myristoylation of NCSs have been discussed [32]. First, the insertion of the myristoyl group into the lipid bilayer and its function as a membrane anchor. Second, an extrusion mechanism that exposes the myristoyl group upon Ca^{2+} binding of the protein to either insert into the membrane or bind to and activate a target effector. Third, a protein structure stabilizing function of the myristoyl group, which is fully buried in a hydrophobic pocket of the protein [18].

Clearly, more structural information is required to better understand the role of the myristoyl moiety of the GCAPs in the course of action of the protein. We have previously studied the structure and dynamics of the myristoyl lipid modification of the GCAP-2 protein bound to lipid membranes [33]. This study provided a first hint that the myristoyl chain is fully inserted into the membrane showing similar structure and dynamics as the surrounding phospholipids. Unfortunately, from this ^{2}H NMR study no information about the N-terminal amino acids in the direct vicinity of the myristoylation was available. For one reason, specific isotopic labeling of proteins with reasonable yields remains a large challenge in structural biology. On the other hand, fully $^{13}C/^{15}N$-labeled membrane-associated proteins usually do not provide sufficient resolution and sensitivity for efficient solid-state NMR structure determination. Therefore, we have decided to continue our investigation of the structure and dynamics of membrane bound GCAP-2 using myristoylated N-terminal peptides. Indeed, in the last 15 years a number of studies have shown that that studies of lipidated peptides helped in understanding some of the open questions with regard to membrane binding of proteins via lipid chains [34–38].

In the current paper, we present our data on the structure and the dynamics of a 19 amino acid peptide representing the myristoylated N-terminus of GCAP-2 bound to lipid membranes (DMPC liposomes) by solid-state NMR. We use a combination of methods to study (i) the secondary structure of several amino acids in the membrane bound peptide fragment; (ii) the interaction of the GCAP-2 molecule with the membrane; (iii) the amplitudes of molecular motions in these residues; and (iv) the structure and dynamics of the myristoyl moiety attached to the N-terminal Gly residue.

2. Material and methods

2.1. Materials

The glycerophospholipids 1,2-dimyristoyl-*sn*-glycero-3-phosphocholine (DMPC), 1,2-dimyristoyl-*sn*-glycero-3-phosphocholine-1,1,2,2-d_4-N,N,N-trimethyl-d_9 (DMPC-d_{13}), 1,2-dimyristoyl-d_{54}-*sn*-glycero-3-phosphocholine (DMPC-d_{54}), and 1,2-dimyristoyl-d_{54}-*sn*-glycero-3-phosphocholine-1,1,2,2-d_4-N,N,N-trimethyl-d_9 (DMPC-d_{67}) were purchased from Avanti Polar Lipids (Alabaster, AL) and used without further purification.

Four myristoylated peptides with an amino acid sequence identical to the first 19 amino acids of GCAP-2 (myr-GQQFSWEEA EENGAVGAAD) were synthesized using standard Fmoc solid phase peptide synthesis. The labeling pattern of the respective peptides is shown in Scheme 1.

2.2. Sample preparation

To prepare multilamellar vesicles (MLVs), the phospholipids were suspended in aqueous buffer solution (50 mM HEPES, 10 mM NaCl, pH 7.4). After 10 freeze–thaw cycles, the solution was extruded 10 times through two polycarbonate filters of 100 nm pore size (Millipore, Billerica) at 37 °C using a LIPEX thermo stated extruder (Biomembranes, Vancouer, BC, Canada) [39]. The peptides were dissolved in the

myr-GQQF**S**WEEA**E**ENGAV**G**A**A**D*

myr-**G**QQFSWEE**A**EENGA**V**GAAD

myr-GQQ**F**SWEEAEEN**GA**VGAAD

myr-GQQFSWEEAEENGAVGAAD

* U-^{13}C, ^{15}N labeled amino acids and a perdeuterated myristoyl moiety are marked with bold underscored letters.

Scheme 1. N-terminal GCAP-2 peptides and labeling schemes.

same buffer solution and added to the LUVs to obtain a final peptide to lipid molar ratio of 1:20. After incubation for at least 12 h with freeze–thaw cycles every 2 h the mixture was ultracentrifuged at 150,000 × *g* for 50 min. The resulting pellet was lyophilized and then rehydrated to a final water concentration of 35 % (w/v) with D_2O or deuterium-depleted water for the ^{1}H and ^{2}H NMR measurements, respectively. For equilibration, the sample was frozen, thawed, stirred and gently centrifuged several times. The supernatant from the ultracentrifugation was analyzed by standard protein determination assays. From the difference between the initial GCAP-2 concentration and the peptide concentration determined after centrifugation, the amount of bound peptide was determined.

2.3. ^{13}C MAS NMR spectroscopy

All ^{13}C experiments were carried out on a Bruker Avance 750 NMR spectrometer operating at a resonance frequency of 749.8 MHz for ^{1}H and 188.5 MHz for ^{13}C. ^{13}C cross-polarization magic angle spinning (CP MAS) NMR spectra were acquired at (303 ± 0.1) K using a double resonance MAS probe equipped with a 4-mm spinning module. The ^{1}H and ^{13}C 90° pulse lengths were 4 and 5 μs, respectively, and a CP contact time of 700 μs was used. A MAS frequency of (7000 ± 2) Hz was maintained by the pneumatic control unit. For heteronuclear decoupling a TPPM15 pulse sequence with radiofrequency field strength of 65 kHz was applied during the detection period [40]. The ^{13}C chemical shifts were externally referenced to the Gly ^{13}CO signal (176.45 ppm relative to TMS) [41].

Spin diffusion experiments were carried out using the published pulse sequence [42]. For this experiment, a GCAP-2 molecules with deuterated myristoyl chain and U-^{13}C/^{15}N labeled Gly_1, Phe_4, Ala_9, and Val_{15} was bound to a headgroup deuterated DMPC-d_{13} membrane. In such a membrane, ^{1}H spin diffusion can only originate from the lipid chains or glycerol region since the deuterated lipid headgroup or D_2O from the hydration shell are not excited by the first pulse on the ^{1}H channel. A long T_2 filter of 6 ms was applied to relax the single quantum coherences of the peptide. Spin diffusion times of 0, 50, 100, 200, 400, and 900 ms were probed. Data points were corrected for T_1 relaxation and normalized to the 900 ms value.

The ^{1}H–^{13}C heteronuclear correlation (HetCor) spectra [43] were measured using the same parameters as for ^{13}C CP MAS spectra. ^{1}H chemical shifts were referenced to the DMPC-glycerine-G2 protons at 5.31 ppm relative to TMS [44]. ^{13}C–^{13}C proton driven spin diffusion spectra [45] were acquired using a mixing time of 500 ms (all other parameters as above).

The strength of the ^{13}C–^{1}H dipolar couplings was measured using the constant time dipolar and chemical shift (DIPSHIFT) pulse sequence [46]. ^{1}H–^{1}H homonuclear decoupling was achieved by the MREV-8 sequence [47] using a decoupler field of 100 kHz. The MAS frequency was (5000 ± 2) Hz. All other parameters were identical to the ^{13}C CP MAS NMR measurements. The dipolar-induced signal decay is periodic with the rotor period, so it was only necessary to acquire the signal over one rotor period. The resulting spectra were only Fourier transformed in the direct dimension and the dipolar dephased signal for each resolved peak was extracted and simulated to obtain the dipolar coupling. Simulations were carried out as described in Hong et al. [48]. Powder averaging was performed in 1° increments for the α and β Euler angles.

C–H order parameters were determined by dividing the measured dipolar coupling by the rigid limit value for the C–H dipolar coupling. The rigid limit values were experimentally obtained from measurements of crystalline amino acid preparations: CH (Ala Cα, 11.5 kHz), CH_2 (Gly Cα, 12.8 kHz), and CH_3 (Ala Cβ, 18.0 kHz) [49].

2.4. ^{2}H solid-state NMR

All ^{2}H experiments were carried out on a Bruker Avance 750 NMR spectrometer operating at a resonance frequency of 115.1 MHz for ^{2}H. The ^{2}H NMR spectra were acquired at (303 ± 0.1) K with a phase-cycled quadrupolar echo sequence [50]. The two 3 μs ^{2}H 90° pulses separated by a 60 μs delay and a recycle delay of 1 s were used. Prior to dePaking of the ^{2}H NMR spectra of the GCAP-2 peptide with a deuterated myristoyl moiety, a small isotropic fraction was subtracted from the NMR spectrum. The resulting ^{2}H powder spectra were dePaked using the algorithm of McCabe und Wassall [51]. Smoothed chain order parameters were calculated according to Lafleur et al. [52]. The Pake doublets were assigned to the carbons consecutively according to their increasing quadrupolar splitting.

The ^{2}H relaxation rates for the decay of Zeeman order (R_{1Z}: spin-lattice relaxation rate) were measured using a phase-cycled inversion-recovery quadrupolar echo pulse sequence with 13 delays between 1 ms and 2.5 s and a relaxation delay of 2 s. All other parameters were the same as for recording the ^{2}H NMR spectra.

2.5. ^{31}P NMR

All ^{31}P NMR spectra were measured using a DRX-600 NMR spectrometer (Bruker, Karlsruhe, Germany) operating at a ^{31}P resonance frequency of 242.8 MHz using a 5-mm double resonance solution NMR probe. A Hahn-echo pulse sequence with a 7 μs 90° pulse, a delay of 50 μs between the pulses, a spectral width of 100 kHz and a relaxation delay of 2 s were used. Low-power broadband ^{1}H decoupling was applied during acquisition. To obtain the chemical shift anisotropy ($\Delta\sigma$) the resulting spectra were simulated using Mathcad 2001 (MathSoft Engeneering and Education, Cambridge, MA).

3. Results

3.1. ^{31}P NMR spectroscopy

To confirm that the phospholipid membranes were in the liquid crystalline phase and that membrane binding of the peptide does not disturb the bilayer we measured ^{31}P NMR spectra of DMPC-d_{54} in the presence and in the absence of GCAP-2 peptides (spectra not shown). For pure DMPC-d_{54} MLVs, a value of $\Delta\sigma$ = (46.4 ± 1.0) ppm for the span of the axially symmetric ^{31}P tensor was obtained. In the presence of GCAP-2 peptides, $\Delta\sigma$ remains unchanged (46.8 ± 1.0 ppm).

Obviously, membrane binding of the peptide does not disturb the liquid crystalline phase and the headgroup orientation and mobility of the DMPC membrane.

3.2. Structure and dynamics of the myristoyl moiety and the surrounding lipids of the host membrane

We used ^{2}H solid-state NMR to investigate the structure and the dynamics of the myristoyl moiety of GCAP-2 and the lipids of the surrounding membrane. As the host membrane, DMPC liposomes were chosen, this means that the lipid chain of GCAP-2 and the lipid chains of the membrane of the host matrix were identical. It has been demonstrated earlier that GCAP-2 shows a stronger binding to DMPC liposomes compared to mixed lipid membranes [33]. Although DMPC is not as physiologically relevant as unsaturated mixtures of lipids with varying headgroups, the ^{13}C NMR measurements of the current study necessitated the deuteration of the lipids, which is only available for DMPC.

To examine the influence of the peptide on the structure and dynamics of the host membrane, we studied DMPC-d_{54} multilamellar liposomes in the absence and presence of GCAP-2 peptides. Furthermore, we made use of a GCAP-2 peptide with a deuterated myristoyl moiety incubated with nondeuterated DMPC liposomes to investigate the myristoyl moiety as well. The measured ^{2}H solid-state NMR spectra are shown in Fig. 1. All spectra are well resolved showing the typical superposition of Pake doublets. The spectral width of about 30 kHz is comparable among all three spectra and typical for lipid chains in a liquid crystalline phase state. Interestingly, the myristoyl moiety also shows this characteristic NMR spectrum indicating that it is well incorporated into the DMPC membrane bilayer.

To analyze the spectra in more detail, smoothed order parameter profiles were calculated (Fig. 2). Compared to pure DMPC-d_{54} liposomes, the order parameters of DMPC-d_{54} in the presence of GCAP-2 peptides were slightly lower. Somewhat lower order parameters were observed for the myristoyl moiety of the membrane bound GCAP-2 peptide. Whereas the biggest difference was observed in the middle of the chains, the order parameters are close at the top and at the bottom of the chains. All these results indicate that the myristoyl moiety is incorporated into the membrane bilayer and that the packing and the dynamics of these chains are rather similar to the surrounding lipids of the DMPC host membrane.

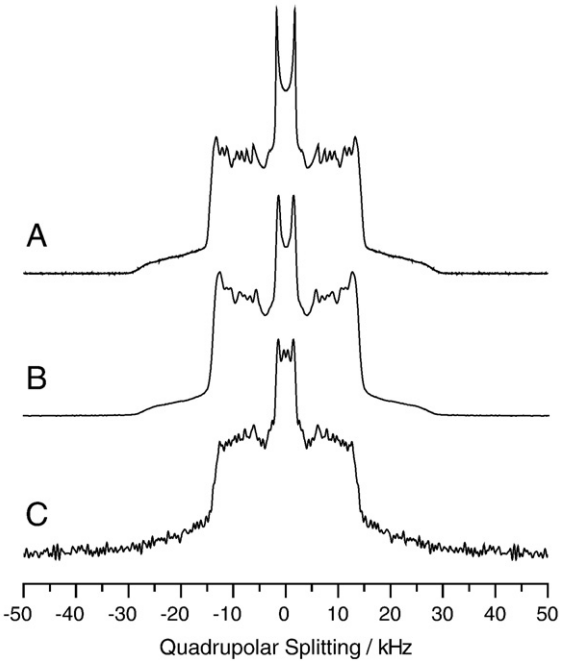

Fig. 1. 115.1 MHz ^{2}H NMR powder spectra of (A) DMPC-d_{54}, (B) DMPC-d_{54} in the presence of GCAP-2 peptides, and (C) the deuterated myristoyl moiety of the GCAP-2 peptides in DMPC liposomes, recorded at a temperature of 30 °C. The peptide concentration was 4.8 mol% and the samples contained 35% (w/v) deuterium-depleted water. A total of 2048, 1024, and 10496 transients was acquired for spectra shown in (A), (B), and (C), respectively.

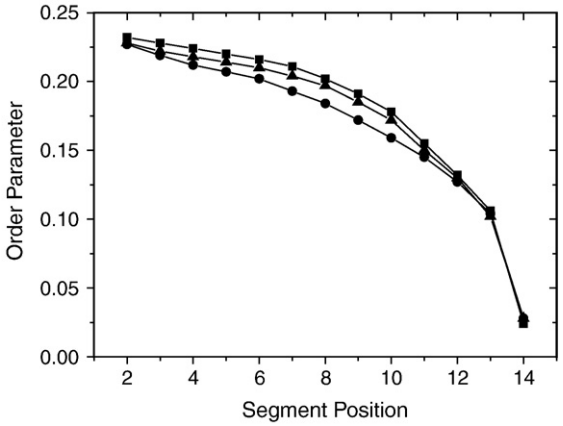

Fig. 2. Smoothed chain order parameter $|S_{CD}^{(i)}|$ profiles for DMPC-d_{54} liposomes in the absence (■) and in the presence (▲) of GCAP-2 peptides and for the myristoyl moiety of GCAP-2 (●) as a function of the chain segment position determined from the ^{2}H NMR spectra shown in Fig. 1. Note that the myristoyl moiety has a similar order profile indicating that its packing and dynamics are similar to the lipids of the DMPC host membrane.

From the smoothed order parameter profiles the lengths (L_C^*) of the myristoyl chains were calculated using the mean-torque model [53,54]. For the myristoyl moiety of the GCAP-2 peptide incorporated into the membrane a chain length of 10.4 Å was found. For the DMPC, the chain length was 10.6 Å in the absence and 10.5 Å in the presence of GCAP-2 peptides.

We further investigate the dynamics of the lipid chains by measuring the Zeeman order ^{2}H NMR relaxation rates (R_{1Z}) for each carbon position. Empirical studies revealed that the relaxation rate often exhibits a linear dependence on the square of the order parameter for saturated phospholipid membranes [55]. Fig. 3 shows such square law plots obtained for DMPC-d_{54} liposomes in the presence and in the absence of GCAP-2 peptides as well as for the myristoyl moiety of GCAP-2. The square law plots are very similar for DMPC in the absence and presence of GCAP-2. The plot of the myristoyl moiety of GCAP-2 is also linear but shows a slightly steeper slope. Altogether, these results indicate that the flexibility of DMPC

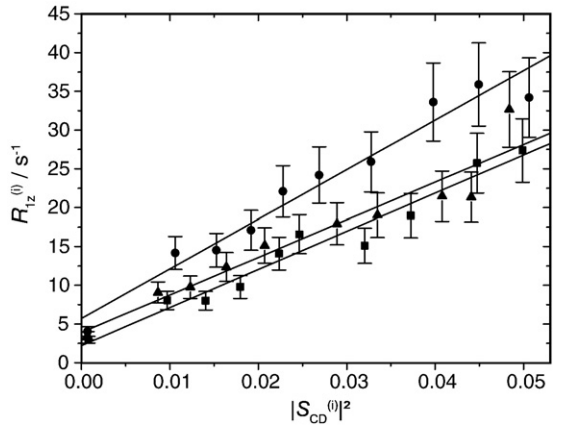

Fig. 3. Relaxation rates $R_{1Z}^{(i)}$ vs. squared order parameters $|S_{CD}^{(i)}|^2$ for DMPC-d_{54} liposomes in the absence (■) and in the presence (▲) of GCAP-2 peptides and for the myristoyl moiety of the peptide (●). The plots indicate that the flexibility of DMPC lipids is not influenced by the peptides; however, the myristoyl moiety of the membrane bound GCAP-2 peptide is slightly more flexible.

lipids is not influenced by the peptides; however, the myristoyl moiety of the membrane bound GCAP-2 peptide is slightly more flexible.

3.3. The secondary structure of membrane bound N-terminal GCAP-2 peptide

The ^{13}C isotropic chemical shift of Cα and Cβ atoms, especially the reference-independent difference Cα–Cβ is a sensitive marker for the secondary structure [56,57]. So we investigated the secondary structure of membrane bound GCAP-2 peptides by measuring the ^{13}C CP MAS NMR spectra as shown in Fig. 4. These spectra were excited via cross-polarization. Due to the choice of labeled amino acids, the assignment of the resolved peaks in the spectra could be done on the basis of literature values [58].

To confirm the assignments of the ^{13}C NMR signals and to also obtain the structurally relevant peak assignment of the Hα signals, ^{1}H–^{13}C HetCor experiments were carried out. A representative HetCor spectrum recorded without any homonuclear decoupling during the evolution of the ^{1}H chemical shift is shown in Fig. 5. Additionally, the assignment of the Ser_5Cα and Glu_{10}Cα signals in Fig. 4A were checked by a 2D ^{13}C–^{13}C proton driven spin diffusion experiment (data not sown).

We studied the secondary structure of 10 amino acids of the GCAP-2 peptide scattered over the entire sequence. Table 1 summarizes the measured isotropic Hα, Cα, and Cβ chemical shifts and presents the predicted secondary structure. All chemical shifts are in agreement with random coil conformation of the membrane-associated peptide. With the only exception of Ser_5 Cα, we have not found any evidence for either α-helical or β-sheet conformation. Although not all residues in the sequence were subjected to the secondary structure analysis, the maximum information gap amounted to three consecutive residues. This is too little to assume that a secondary structure element was formed. Therefore, it is safe to conclude that the entire membrane-associated peptide assumed a random coil conformation.

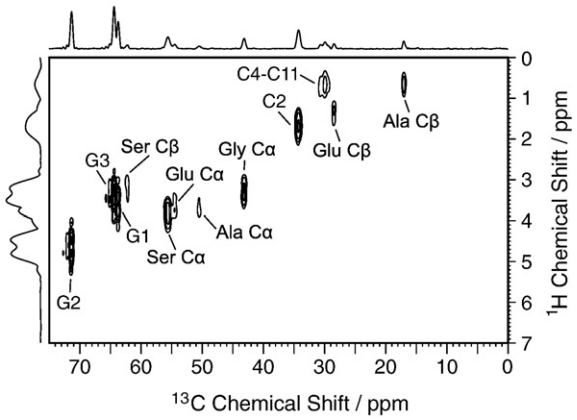

Fig. 5. Contour plot of a ^{1}H–^{13}C heteronuclear correlation spectrum of GCAP-2 peptide (myr-GQQFSWEEAEENGAVGAAD) bound to DMPC-d_{67} liposomes, measured at 30 °C, with a MAS frequency of 7 kHz. No homonuclear decoupling was applied during the evolution of the ^{1}H chemical shift. The samples contained 35 % (w/v) D_2O. A total of 488 transients was acquired in each t_1 increment.

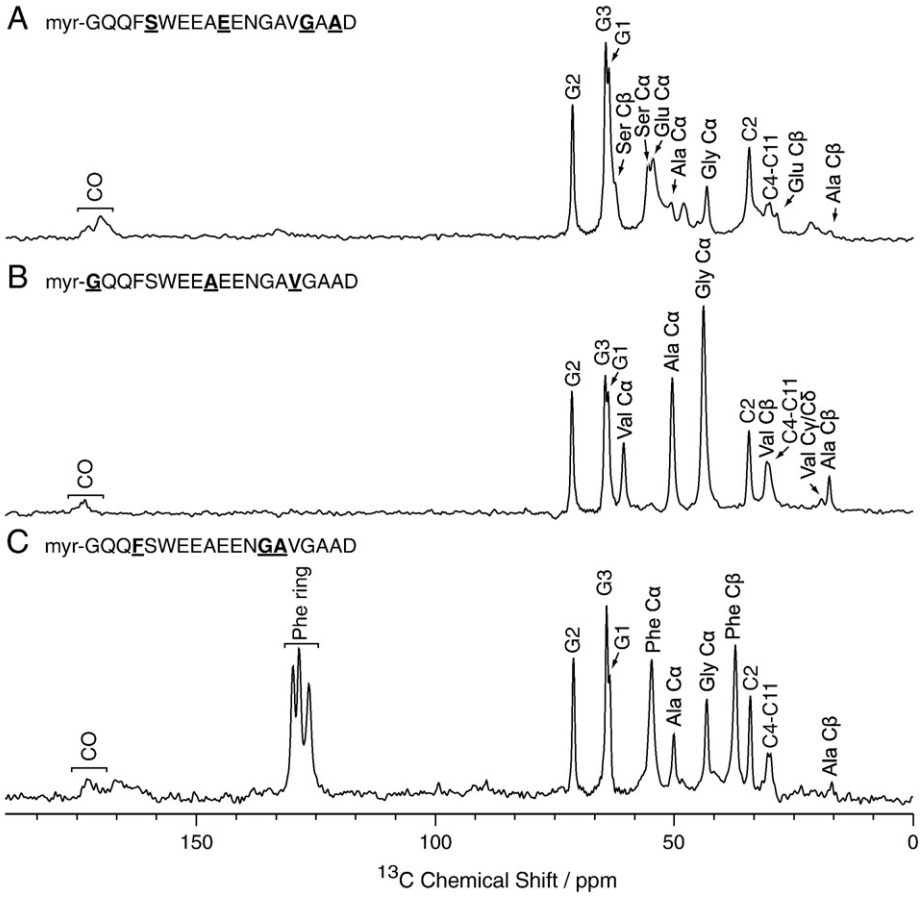

Fig. 4. Proton decoupled 188.5 MHz ^{13}C CP MAS NMR spectra of GCAP-2 peptides bound to DMPC-d_{67} membranes, acquired at 30 °C, with a MAS frequency of 7 kHz. The peptide to lipid molar ratio was 1:20. The samples contained 35 % (w/v) D_2O. Peptide signals are assigned using the three letter code. Lipid signals that were not or insufficiently deuterated are also assigned. The peptide sequence and labeling schemes are also given. ^{13}C labeled amino acids were underlined and highlighted in bold letters. The number of scans for each ^{13}C NMR spectrum was 2048, 3072, and 1024 for A–C, respectively.

3.4. Membrane interaction of GCAP-2 peptides

After establishing that membrane-associated GCAP-2 peptides assume a random coil structure in the membrane, we investigated whether the polypeptide chain was associated with the membrane or freely mobile in the aqueous phase. To this end, we used an experiment that exploits spin diffusion that originates in the lipid membrane and proceeds into the membrane-associated peptide [42]. A myristoylated GCAP-2 peptide was synthesized that featured ^{13}C isotopic labels at Gly_1, Phe_4, Ala_9, and Val_{15} and a deuterated myristoyl moiety. To ensure that ^{1}H spin diffusion would originate from the glycerol/phospholipid chains, we studied the peptide in a DMPC-d_{13} membrane, which is deuterated in the headgroup, in the presence of D_2O. Spin diffusion build-up curves from the membrane into the peptide as a function of mixing time are shown in Fig. 6. For Val_{15}, no intensity could be detected within experimental error, suggesting that the C-terminal part of the peptide is not in contact with the membrane. For the other labels (Gly_1, Phe_4, Ala_9), spin diffusion build up is detected indicating that these residues are in contact with the membrane interface region. Within experimental error, these spin diffusion build-up curves are rather similar suggesting that the amino acids up to residue 9 are in contact with the membrane. Given the quality of the experimental data, a more quantitative analysis of the spin diffusion results was not possible. As seen from Fig. 6, the built up has not reached a plateau value after 900 ms. As suggested from the good resolution of the ^{1}H–^{13}C HetCor experiments, the lipidated peptide is rather mobile on the membrane surface, which decreases the spin diffusion efficiency. Furthermore, molecular mobility reduces the efficiency of the short CP or Lee-Goldburg-CP, respectively. A relatively long T_2 filter time of 6 ms had to be used to fully relax the magnetization of the peptide, which further decreased the sensitivity of the experiment.

In spite of these technical difficulties, which prevented a quantitative analysis of the spin diffusion experiment, the interesting result emerged that the peptide segments at least up to Ala_9 must be in contact to the lipid membrane interface while the second half of the peptide is more localized in the aqueous phase.

3.5. Dynamics of membrane bound GCAP-2 peptides

The previous experiments suggested a high mobility of the membrane-associated GCAP-2 peptide. Therefore, we quantitatively studied the dynamics of the molecule at the membrane to gain further insight into the membrane binding of the amino acids adjacent to the myristoylation.

We used the DIPSHIFT pulse sequence to determine the strength of the ^{1}H–^{13}C dipolar couplings along the backbone and the side chains of the membrane bound GCAP-2 peptides. Fast anisotropic molecular motions partially average these couplings. This allows determining the spatial restriction of the motions of the C–H bond vectors, which

Table 1
Isotropic chemical shifts for the Cα, Cβ, and Hα atoms (in ppm), difference of the chemical shifts (Cα–Cβ) and predicted secondary structure.

	Cα	Cβ	Cα–Cβ	Hα	Secondary structure
Gly_1	43.8 ± 0.5	–	–	4.1	random coil
Phe_4	54.6 ± 0.5	37.1 ± 0.5	17.5 ± 0.5	4.6	random coil
Ser_5	55.5 ± 0.1	62.2 ± 0.1	-6.7 ± 0.1	4.4	random coil / β-sheet
Ala_9	50.4 ± 0.5	17.5 ± 0.1	32.9 ± 0.5	4.3	random coil
Glu_{10}	54.5 ± 0.1	28.6 ± 0.1	25.9 ± 0.1	4.1	random coil
Gly_{13}	43.3 ± 0.4	–	–	4.0	random coil
Ala_{14}	49.9 ± 0.4	17.0 ± 0.4	32.9 ± 0.4	4.4	random coil
Val_{15}	60.6 ± 0.1	30.5 ± 0.3	30.1 ± 0.3	4.1	random coil
Gly_{16}	43.2 ± 0.1	–	–	4.1	random coil
Ala_{18}	50.7 ± 0.1	17.4 ± 0.2	33.3 ± 0.2	4.4	random coil

All chemical shifts are measured at a temperature of 30 °C and referenced relative to TMS.

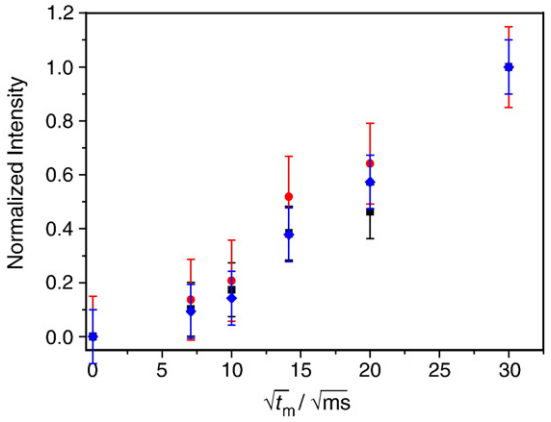

Fig. 6. Spin diffusion build-up curves as a function of mixing time (t_m) for Gly_1Cα (■), Phe_4Cα (♦) and Ala_9Cα (●), of the GCAP-2 peptide bound to DMPC-d_{13} membranes. Error bars represent the noise level in the ^{13}C spin diffusion spectra.

can be expressed by an order parameter S that is defined as the ratio of the motional averaged and the full dipolar coupling. Fig. 7 shows the experimental order parameters for the membrane bound GCAP-2 peptide. The order parameters along the polypeptide chain do not show a conclusive increase or decrease along the polypeptide chain and are relatively low indicating that the membrane bound peptide undergoes large-amplitude molecular motions. For the Ala_{14} Cβ and Ala_{18} Cβ no order parameter could be determined because the signal intensity was too low. Also for Ser_5 Cβ, no order parameter could be obtained because the signal overlapped with the lipid G1 signal. Furthermore, the Glu_{10} Cβ signal was influenced too strongly by the lipid C4-C11 signal to determine the order parameter correctly.

The order parameters obtained for the Cβ atoms are typically lower then for the neighboring Cα atoms, which indicates that the amplitude of motions increases along the side chains. An exception is the Phe_4 Cβ, which has a higher order parameter then its corresponding Cα site. Interestingly, the ring atoms show very low order parameters, which could be a result of fast two-site jump motions.

With the exception of Glu_{10}, the Cα order parameters fall between ~0.2 and 0.45. This would be in agreement that the entire polypeptide chain is located in the membrane surface/interface area. It is conceivable that the charged Glu residues are repelled from the

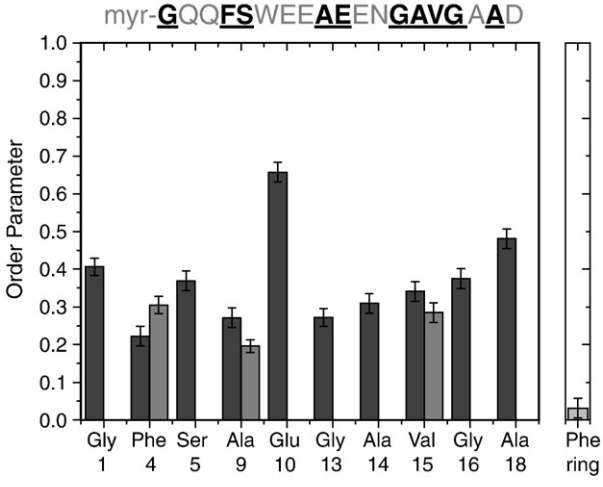

Fig. 7. ^{1}H–^{13}C order parameters along the backbone and the side chains of the membrane bound GCAP-2 peptide. Dark gray bars correspond to order parameters determined for Cα, light gray bars for Cβ. The sequence is shown above. ^{13}C labeled amino acids are marked with bold black letters.

surface due to Born repulsion, which could lead to somewhat higher molecular order.

4. Discussion

All members of the NCS protein family are myristoylated, however, the biological function of these covalently attached groups appears to vary [32]. Here, we have studied structure, dynamics, and membrane binding of a myristoylated peptide from the N-terminus of GCAP-2 using solid-state NMR spectroscopy. Although the intramolecular interactions within the GCAP protein are not represented, the advantage of using a peptide model is that all measurements could be carried out in the presence of lipid bilayer membranes, which was not the case in either the crystal or the solution NMR studies on GCAPs. While the structure of the soluble protein part would most likely not be influenced by membrane binding, an important question regards the myristoylation and the adjacent residues on the N-terminus of the protein. Since solution NMR or X-ray methods often fail for membrane-associated proteins, solid-state NMR was employed here. This methodology necessitated the use of shorter peptides for resolution and sensitivity reasons. Nevertheless, the lipid-modified membrane anchor of a protein can be treated rather independently from the soluble rest of the molecule. This is suggested from structural data for the Ras protein, which has demonstrated that lipidated peptides representing the membrane anchor of the molecule exhibit akin structural and dynamic features compared to the entire membrane-associated Ras protein [30,34]. In particular, our data on the structure and dynamics of the myristoylation of the GCAP-2 peptide show a very similar structure and dynamics as found for the full-length protein [33], which suggests that the results from the peptide model of the current study have relevance for the GCAP-2 protein. With this prerequisite we continued to study structure, membrane topology, and dynamics of the amino acids adjacent to the myristoylation of GCAP-2 in the membrane.

First, we investigated the secondary structure of a membrane bound N-terminal peptide of GCAP-2 (amino acids 1–19) by measuring the isotropic chemical shifts of the Hα, Cα, and Cβ atoms. Although the solution NMR structure of non-myristoylated GCAP-2 solved by Ames et al. [1], shows a short α-helix in the N-terminal region (residues 7–11), we could not confirm any secondary structure in the N-terminal peptide of membrane bound GCAP-2 peptides. All measured ^{13}C chemical shifts predict a random coil conformation. Possibly, the α-helix is only formed when interactions with the rest of the protein occur or is induced by the solution condition in the absence of membranes. But strong interactions between the N-terminus of GCAP-2 and the rest of the protein seem to be unlikely considering the high flexibility of this protein segment shown in the solution NMR data [1]. Furthermore, the short α-helix in the N-terminal segment is not compatible with membrane binding. The amino acid sequence of this helix is Trp-Glu-Glu-Ala-Glu. In a helical wheel presentation, the negatively charged amino acids would point into all directions rendering the helix very hydrophilic. Such a helix can not bind to the membrane surface. Born repulsion between the fixed charges on the Glu residues and the membrane surface of low dielectric constant would repel this structural arrangement from the membrane [59].

Second, the spin diffusion experiments conducted here suggest that the polypeptide chain at least until Ala_9 interacts with the membrane interface. This is in agreement with the absence of the short α-helix in the N-terminus of GCAP-2. Apparently, the myristoylation together with the hydrophobic sidechains (Phe, Trp) tie the peptide to the membrane surface where hydrogen bonds between the peptide backbone and the carbonyl and phosphate groups of the lipid molecules can be formed. In such a structural arrangement, the negatively charged sidechains of the Glu residues can point away from the membrane minimizing the energy penalty arising from Born repulsion. Typically, nonhydrogen bonded polypeptides cannot cross the membrane [60], but the localization at the surface or in the lipid–water interface of the membrane offers various ways of interaction with polar and apolar lipid segments as well as hydrogen bond formation with the carbonyl and phosphate groups from the lipids. Such interactions can generate sufficient free energy for such a structural arrangement.

Third, we studied the molecular dynamics of the membrane-associated GCAP-2 peptide. These molecules are highly dynamic in the membrane environment as shown by the low order parameters. This high mobility expressed by low order parameters are also in agreement with a random coil conformation of the peptide and can explain the good resolution in the ^1H dimension of the ^1H–^{13}C HetCor experiments. Due to the high mobility, the dipolar couplings that broaden the ^1H NMR spectra are reduced and could efficiently average out by MAS. Low order parameters, i.e., high mobility was also found for the membrane-associated Ras protein, although this molecule features two lipid modifications [29,61]. Apparently, membrane binding through covalently attached lipid chains also renders the peptide chain rather mobile as is the liquid crystalline lipid membrane.

Fourth, we investigated the structure and the dynamics of the myristoyl moiety of the membrane bound GCAP-2 peptide. Our results show that the myristoyl chain of the peptide is fully incorporated into the phospholipid bilayer, whereas the order parameter, the chain length, and the square law plot are comparable to the lipid chains of the DMPC host matrix. This confirms previous studies on the full-length GCAP-2 protein [33]. This result also means that the N-terminal peptide segment is placed into the lipid water interface of the membrane, which is confirmed by our spin diffusion studies. This situation is for example also found in the Ras peptide [34]. Nonetheless, the lipid modifications of Ras were found to be more mobile than the lipid chains of the host matrix as a consequence of the chain length adaptation to the host membrane [54]. For the GCAP-2 peptide with its myristoyl moiety and a DMPC host matrix, there is no need for a largely altered mobility of the myristoyl moiety to match the average length of the host matrix. Consequently, we found that the mobility of the myristoyl moiety is comparable to the mobility of the DMPC lipid chains. Furthermore, all determined parameters concerning the structure and the dynamics of the myristoyl moiety of the peptide are in agreement with those for the myristoyl moiety of the whole GCAP-2 protein in DMPC membranes [33].

Former studies on lipid modified peptides revealed that each methylene group of the lipid chain that partitions into a lipid membrane contributes −3.45 kJ/mol to the Gibbs free energy of the membrane binding [62]. The unitary Gibbs free energy for partitioning a lipid acid chain into *n*-heptane can be estimated by $\Delta G^0{}_u = (17.81 - 3.45\ n_C)$ kJ/mol and also includes a term for the enthalpy penalty (17.81 kJ/mol) [62]. Using this model, for the myristic acid on the GCAP-2 peptide, a Gibbs free energy for membrane partitioning of ~−27 kJ/mol arises. Together with the contribution from the highly hydrophobic Phe and Trp residues, a favorable free energy for membrane binding of $\Delta G^0{}_u \approx$-40 kJ/mol is estimated. Following the simple model used by Vogel et al. [33] to understand the contribution of the myristoyl moiety to the membrane binding of the whole GCAP-2 protein, a Gibbs free energy of ~-40 kJ/mol results in ~90% bound peptide. Routinely, we determined the fraction of DMPC-bound peptide in a centrifugation assay. Typically, about 75% of GCAP-2 was membrane bound under the conditions used in our experiments (data not shown). In good agreement with this crude thermodynamic estimation, the myristoyl moiety is inserted into the membrane and the Gibbs free energy of this insertion can fully explain the peptide binding to the membrane. This may also suggest that the hydrophobic residues Phe_4 and Trp_6 are not permanently membrane inserted, which also agrees with the high mobility we found for Phe_4. Therefore, the myristoyl moiety should play an important role in membrane binding at least for the peptide.

Clearly, the biophysical data of the current and a previous study [33] show that the myristoylation of GCAP-2 is inserted into the membrane. This would agree with the function of that chain as a membrane anchor. Interestingly, former biochemical and biophysical studies have shown that the myristoyl moiety is important for the activation of the GC, but is not essential for membrane binding [16], which would support a model, where the myristic acid chain switches between a membrane and a protein imbedded state ("switch model"). At this point, it must remain open if the myristoylation of GCAP-2 may be extracted from the membrane to play a role in the activation of the GC. Clearly, interaction studies of GCAP-2 with the GC will shed light on this important issue but our work suggests that the myristoylation of GCAP-2 represents an essential contribution of the membrane binding energy of the protein. It is also possible, that the myristoyl moiety of GCAP-2 may direct the protein to the right membrane compartment. Clearly, interaction studies between GCAP proteins and peptides with the GC or segments of this protein are necessary to fully understand the role of the myristoyl moiety of the GCAPs. These studies represent the next steps in our activity in this field.

Acknowledgements

This work was supported by the Deutsche Forschungsgemeinschaft (DFG, HU 720/10-1) and the "Exzellenznetzwerk Biowissenschaften" funded by the federal state of Sachsen-Anhalt. We also thank the DFG and the Experimental Physics Institutes of the University of Leipzig for providing measuring time on the Avance 750 MHz NMR spectrometer. The GCAP peptides were synthesized at the IZKF core unit of the Medical Faculty at the University of Leipzig.

References

[1] J.B. Ames, A.M. Dizhoor, M. Ikura, K. Palczewski, L. Stryer, Three-dimensional structure of guanylyl cyclase activating protein-2, a calcium-sensitive modulator of photoreceptor guanylyl cyclases, J. Biol. Chem. 274 (1999) 19329–19337.
[2] A.M. Dizhoor, E.V. Olshevskaya, W.J. Henzel, S.C. Wong, J.T. Stults, I. Ankoudinova, J.B. Hurley, Cloning, sequencing, and expression of A 24-KDa Ca^{2+}-binding protein activating photoreceptor guanylyl cyclase, J. Biol. Chem. 270 (1995) 25200–25206.
[3] W.A. Gorczyca, A.S. Polans, I.G. Surgucheva, I. Subbaraya, W. Baehr, K. Palczewski, guanylyl cyclase-activating protein—a calcium-sensitive regulator of phototransduction, J. Biol. Chem. 270 (1995) 22029–22036.
[4] F. Haeseleer, I. Sokal, N. Li, M. Pettenati, N. Rao, D. Bronson, R. Wechter, W. Baehr, K. Palczewski, Molecular characterization of a third member of the guanylyl cyclase-activating protein subfamily, J. Biol. Chem. 274 (1999) 6526–6535.
[5] K. Palczewski, I. Subbaraya, W.A. Gorczyca, B.S. Helekar, C.C. Ruiz, H. Ohguro, J. Huang, X.Y. Zhao, J.W. Crabb, R.S. Johnson, K.A. Walsh, M.P. Gray-Keller, P.B. Detwiler, W. Baehr, Molecular-cloning and characterization of retinal photoreceptor guanylyl cyclase-activating protein, Neuron 13 (1994) 395–404.
[6] W.A. Gorczyca, M.P. Gray-Keller, P.B. Detwiler, K. Palczewski, Purification and physiological evaluation of a guanylate cyclase activating protein from retinal rods, Proc. Natl. Acad. Sci. U. S. A. 91 (1994) 4014–4018.
[7] R.D. Burgoyne, J.L. Weiss, The neuronal calcium sensor family of Ca^{2+}-binding proteins, Biochem. J. 353 (2001) 1–12.
[8] Y. Imanishi, G. Li, I. Sokal, M.E. Sowa, O. Lichtarge, T.G. Wensel, D.A. Saperstein, W. Baehr, K. Palczewski, Characterization of retinal guanylate cyclase-activating protein 3 (GCAP3) from zebrafish to man, Eur. J. Neurosci. 15 (2002) 63–78.
[9] R. Stephen, S. Filipek, K. Palczewski, M.C. Sousa, Ca^{2+}-dependent regulation of phototransduction, Photochem. Photobiol. 84 (2008) 903–910.
[10] K.W. Koch, GCAPs, the classical neuronal calcium sensors in the retina. A Ca^{2+}-relay model of guanylate cyclase activation, Calcium Binding Proteins 1 (2006) 3–6.
[11] J.C. Demar, D.R. Rundle, T.G. Wensel, R.E. Anderson, Heterogeneous N-terminal acylation of retinal proteins, Prog. Lipid Res. 38 (1999) 49–90.
[12] R.J. Duronio, D.A. Towler, R.O. Heuckeroth, J.I. Gordon, Disruption of the yeast N-myristoyl transferase gene causes recessive lethality, Science 243 (1989) 796–800.
[13] C.J. Glover, C. Goddard, R.L. Felsted, N-myristoylation of p60src. Identification of a myristoyl-CoA:glycylpeptide N-myristoyltransferase in rat tissues, Biochem. J. 250 (1988) 485–491.
[14] D.A. Towler, S.P. Adams, S.R. Eubanks, D.S. Towery, E. Jacksonmachelski, L. Glaser, J.I. Gordon, Purification and characterization of yeast myristoyl-CoA-protein N-myristoyltransferase, Proc. Natl. Acad. Sci. U. S. A. 84 (1987) 2708–2712.
[15] J.Y. Hwang, K.W. Koch, The myristoylation of the neuronal Ca^{2+}-sensors guanylate cyclase-activating protein 1 and 2, Biochim. Biophys. Acta 1600 (2002) 111–117.
[16] E.V. Olshevskaya, R.E. Hughes, J.B. Hurley, A.M. Dizhoor, Calcium binding, but not a calcium-myristoyl switch, controls the ability of guanylyl cyclase-activating protein GCAP-2 to regulate photoreceptor guanylyl cyclase, J. Biol. Chem. 272 (1997) 14327–14333.
[17] R. Stephen, K. Paiczewski, M.C. Sousa, The crystal structure of GCAP3 suggests molecular mechanism of GCAP-linked cone dystrophies, J. Mol. Biol. 359 (2006) 266–275.
[18] R. Stephen, G. Bereta, M. Golczak, K. Palczewski, M.C. Sousa, Stabilizing function for myristoyl group revealed by the crystal structure of a neuronal calcium sensor, guanylate cyclase-activating protein 1, Structure 15 (2007) 1392–1402.
[19] S. Lim, I. Peshenko, A. Dizhoor, J.B. Ames, Effects of Ca^{2+}, Mg^{2+}, and myristoylation on guanylyl cyclase activating protein 1 structure and stability, Biochemistry 48 (2009) 850–862.
[20] J. Torres, T.J. Stevens, M. Samso, Membrane proteins: the 'Wild West' of structural biology, Trends Biochem. Sci. 28 (2003) 137–144.
[21] D. Huster, Investigations of the structure and dynamics of membrane-associated peptides by magic angle spinning NMR, Prog. Nucl. Magn. Reson. Spectrosc. 46 (2005) 79–107.
[22] T.A. Cross, S.J. Opella, Solid-state NMR structural studies of peptides and proteins in membranes, Curr. Opin. Struct. Biol. 5 (1994) 574–581.
[23] J.H. Davis, M. Auger, Static and magic angle spinning NMR of membrane peptides and proteins, Prog. Nucl. Magn. Reson. Spectrosc. 35 (1999) 1–84.
[24] E. Strandberg, A.S. Ulrich, NMR methods for studying membrane-active antimicrobial peptides, Concepts Magn. Reson. 23A (2004) 89–120.
[25] B. Bechinger, The structure, dynamics and orientation of antimicrobial peptides in membranes by multidimensional solid-state NMR spectroscopy, Biochim. Biophys. Acta 1462 (1999) 157–183.
[26] S. Luca, H. Heise, M. Baldus, High-resolution solid-state NMR applied to polypeptides and membrane proteins, Acc. Chem. Res. 36 (2003) 858–865.
[27] G. Lindblom, G. Grobner, NMR on lipid membranes and their proteins, Curr. Opin. Coll. Int. Sci. 11 (2006) 24–29.
[28] M. Hong, Structure, topology, and dynamics of membrane peptides and proteins from solid-state NMR Spectroscopy, J. Phys. Chem. B 111 (2007) 10340–10351.
[29] L. Brunsveld, H. Waldmann, D. Huster, Membrane binding of lipidated Ras peptides and proteins — The structural point of view, Biochim. Biophys. Acta 1788 (2009) 273–288.
[30] G. Reuther, K.T. Tan, J. Köhler, C. Nowak, A. Pampel, K. Arnold, J. Kuhlmann, H. Waldmann, D. Huster, Structural model of the membrane-bound C terminus of lipid-modified human N-ras protein, Angew. Chem. Int. Ed Engl. 45 (2006) 5387–5390.
[31] T.G. Wensel, Signal transducing membrane complexes of photoreceptor outer segments, Vision Res. 48 (2008) 2052–2061.
[32] L.P. Haynes, R.D. Burgoyne, Unexpected tails of a Ca^{2+}sensor, Nat. Chem. Biol. 4 (2008) 90–91.
[33] A. Vogel, T. Schroder, C. Lange, D. Huster, Characterization of the myristoyl lipid modification of membrane-bound GCAP-2 by H-2 solid-state NMR spectroscopy, Biochim. Biophys. Acta 1768 (2007) 3171–3181.
[34] D. Huster, A. Vogel, C. Katzka, H.A. Scheidt, H. Binder, S. Dante, T. Gutberlet, O. Zschörnig, H. Waldmann, K. Arnold, Membrane insertion of a lipidated ras peptide studied by FTIR, solid-state NMR, and neutron diffraction spectroscopy, J. Am. Chem. Soc. 125 (2003) 4070–4079.
[35] R.M. Peitzsch, S. McLaughlin, Binding of acylated peptides and fatty acids to phospholipid vesicles: pertinence to myristoylated proteins, Biochemistry 32 (1993) 10436–10443.
[36] C.T. Pool, T.E. Thompson, Chain length and temperature dependence of the reversible association of model acylated proteins with lipid bilayers, Biochemistry 37 (1998) 10246–10255.
[37] S. Shahinian, J.R. Silvius, Doubly-lipid-modified protein sequence motifs exhibit long-lived anchorage to lipid bilayer membranes, Biochemistry 34 (1995) 3813–3822.
[38] H.A. Scheidt, D. Huster, Structure and dynamics of the myristoyl lipid modification of Src peptides determined by ^2H solid-state NMR Spectroscopy, Biophys. J. 96 (2009) 3663–3672.
[39] M.J. Hope, M.B. Bally, G. Webb, P.R. Cullis, Production of large unilamellar vesicles by a rapid extrusion procedure. Characterization of size distribution, trapped volume, and ability to maintain a membrane potential, Biochim. Biophys. Acta 812 (1985) 55–65.
[40] A.E. Bennett, C.M. Rienstra, M. Auger, K.V. Lakshmi, R.G. Griffin, Heteronuclear decoupling in rotating solids, J. Chem. Phys. 103 (1995) 6951–6958.
[41] C.R. Morcombe, K.W. Zilm, Chemical shift referencing in MAS solid state NMR, J. Magn. Reson. 162 (2003) 479–486.
[42] D. Huster, X. Yao, M. Hong, Membrane protein topology probed by ^1H spin diffusion from lipids using solid-state NMR spectroscopy, J. Am. Chem. Soc. 124 (2002) 874–883.
[43] C.W. Lee, R.G. Griffin, Two-dimensional $^1H/^{13}C$ heteronuclear chemical shift correlation spectroscopy of lipid bilayers, Biophys. J. 55 (1989) 355–358.
[44] D. Huster, K. Arnold, K. Gawrisch, Investigation of lipid organization in biological membranes by two-dimensional nuclear Overhauser enhancement spectroscopy, J. Phys. Chem. B 103 (1999) 243–251.
[45] N.M. Szeverenyi, M.J. Sullivan, G.E. Maciel, Observation of spin exchange by two-dimensional Fourier transform 13C cross polarization magic-angle spinning, J. Magn. Reson. 47 (1982) 462–475.
[46] M.G. Munowitz, R.G. Griffin, G. Bodenhausen, T.H. Huang, Two-dimensional rotational spin-echo nuclear magnetic resonance in solids: correlation of chemical shift and dipolar interactions, J. Am. Chem. Soc. 103 (1981) 2529–2533.
[47] W.K. Rhim, D.D. Elleman, R.W. Vaughan, Enhanced resolution for solid state NMR, J. Chem. Phys. 58 (1973) 1772–1773.

[48] M. Hong, J.D. Gross, R.G. Griffin, Site-resolved determination of peptide torsion angle Φ from relative orientations of backbone N–H and C–H bonds by solid-state NMR, J. Phys. Chem. 101 (1997) 5869–5874.
[49] D. Huster, L. Xiao, M. Hong, Solid-state NMR investigation of the dynamics of soluble and membrane-bound colicin Ia channel-forming domain, Biochemistry 40 (2001) 7662–7674.
[50] J.H. Davis, K.R. Jeffrey, M. Bloom, M.I. Valic, T.P. Higgs, Quadrupolar echo deuteron magnetic resonance spectroscopy in ordered hydrocarbon chains, Chem. Phys. Lett. 42 (1976) 390–394.
[51] M.A. McCabe, S.R. Wassall, Fast-Fourier-transform DePaking, J. Magn. Reson. B 106 (1995) 80–82.
[52] M. Lafleur, B. Fine, E. Sternin, P.R. Cullis, M. Bloom, Smoothed orientational order profile of lipid bilayers by ^{2}H-nuclear magnetic resonance, Biophys. J. 56 (1989) 1037–1041.
[53] H.I. Petrache, S.W. Dodd, M.F. Brown, Area per lipid and acyl length distributions in fluid phosphatidylcholines determined by ^{2}H NMR spectroscopy, Biophys. J. 79 (2000) 3172–3192.
[54] A. Vogel, C.P. Katzka, H. Waldmann, K. Arnold, M.F. Brown, D. Huster, Lipid modifications of a ras peptide exhibit altered packing and mobility versus host membrane as detected by ^{2}H solid-state NMR, J. Am. Chem. Soc. 127 (2005) 12263–12272.
[55] M.F. Brown, Theory of spin-lattice relaxation in lipid bilayers and biological membranes. ^{2}H and ^{14}N quadrupolar relaxation, J. Chem. Phys. 77 (1982) 1576–1799.
[56] Y.J. Wang, O. Jardetzky, Probability-based protein secondary structure identification using combined NMR chemical-shift data, Protein Sci. 11 (2002) 852–861.
[57] S. Luca, D.V. Filippov, J.H. van Boom, H. Oschkinat, H.J. de Groot, M. Baldus, Secondary chemical shifts in immobilized peptides and proteins: a qualitative basis for structure refinement under magic angle spinning, J. Biomol. NMR 20 (2001) 325–331.
[58] http://www.bmrb.wisc.edu/index.html.
[59] D. Murray, N. Ben-Tal, B. Honig, S. McLaughlin, Electrostatic interaction of myristoylated proteins with membranes: simple physics, complicated biology, Structure 5 (1997) 985–989.
[60] S.H. White, W.C. Wimley, Membrane protein folding and stability: physical principles, Annu. Rev. Biophys. Biomol. Struct. 28 (1999) 319–365.
[61] G. Reuther, K.T. Tan, A. Vogel, C. Nowak, J. Kuhlmann, H. Waldmann, D. Huster, The lipidated membrane anchor of the N-ras protein shows an extensive dynamics as revealed by solid-state NMR, J. Am. Chem. Soc. 128 (2006) 13840–13846.
[62] C. Tanford, The Hydrophobic Effect: Formation of Micelles and Biological Membranes, John Wiley and Sons, New York, 1980.